

Lectures 10-11, T-bone Notes/Slides, 3.054

Trabecular bone

- Foam-like structure
- Exists at ends of long bones — ends have longer surface area than shafts to reduce stress on cartilage at joints; trabecular bone reduces weight
- Also exists in skull, iliac crest (pelvis) — forms sandwich structure — reduces weight
- Also makes up core of vertebrae
- Trabecular bone of interest: (1) osteoporosis (2) osteoarthritis (3) joint replacement

Osteoporosis

- Bone mass decreases with age; osteoporosis — extreme bone loss
- Most common fractures: hip (proximal femur)
vertebrae
- At both sites, most of load carried by trabecular bone
- Hip fractures especially serious: 40% of elderly patients (>65 years old) die within a year (often due to loss of mobility — pneumonia)
- 300,000 hip fractures/year in US
- Costs \$17 billion in 2005

Trabecular bone



Gibson, L. J., and M. F. Ashby. *Cellular Solids: Structure and Properties*. 2nd ed. Cambridge University Press, © 1997. Figures courtesy of Lorna Gibson and Cambridge University Press.

Osteo arthritis

- Degradation of cartilage at joints
- Stress on cartilage affected by moduli of underlying bone
- Cortical bone shell can be thin (e.g. $< 1\text{mm}$)
- Mechanical properties of trabecular bone can affect stress distribution on cartilage

Joint replacement

- If osteoarthritis bad and significant damage to cartilage, may require joint replacement
- Cut end of bone off and insert stem of metal replacement into hollow of long section of bone
- Metals used: titanium, cobalt-chromium, stainless steel
- Bone grows in response to loads on it

Trabecular bone: density depends on magnitude of σ
orientation depends on direction of principal stresses

- Mismatch in moduli between metal and bone leads to stress shielding

	E(GPa)		E(GPa)
Co - 28Cr - Mo	210	Cortical bone	18
Ti alloys	110	Trab. bone	0.01-2
316 Stainless Steel	210		

- After joint replacement, remodeling of remaining bone affected
 - Stiffer metal carries more of load, remaining bone carries less
 - Bone may resorb — can lead to loosening of prosthesis
 - Can cause problems after ~ 15 years
 - Reasons surgeons don't like to do joint replacement on younger patients

Structure of trabecular bone

- Resembles foam: “trabecula” = little beam (Latin)
- Relative density typically 0.05-0.50
- Low density trabecular bone — like open cell foam
- Higher density — becomes like perforated plates
- Can be highly anisotropic, depending on stress field

Trabecular Bone Structure

Images removed due to copyright restrictions.

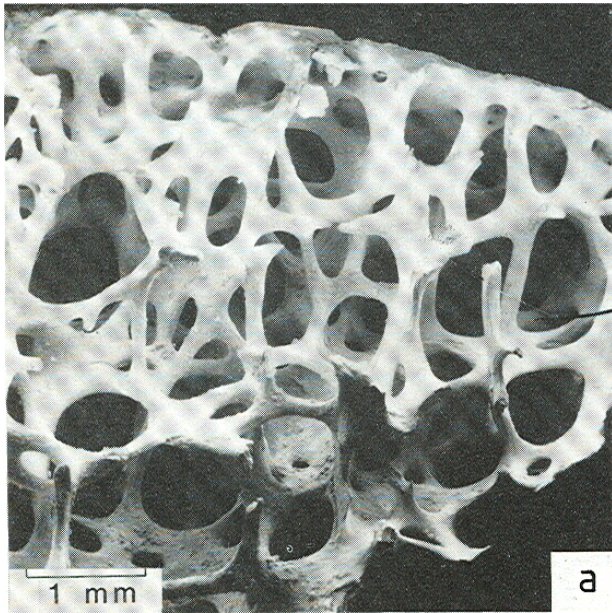
Lumbar spine
11% dense
42 year old male

Femoral head
26% dense
37 year old male

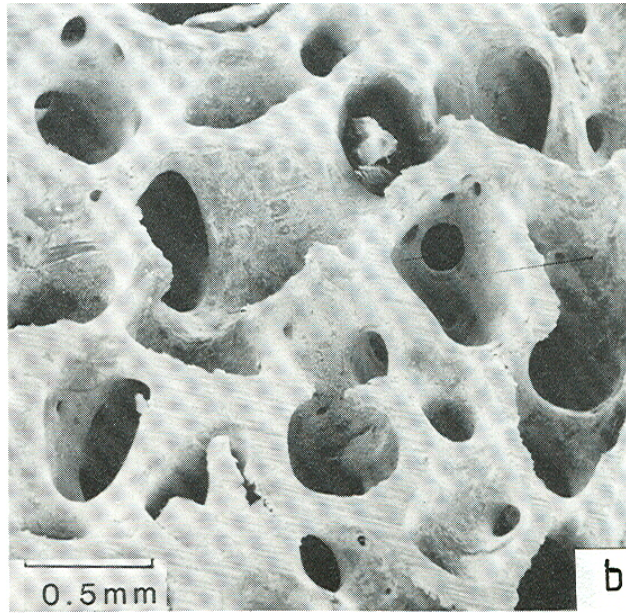
Lumbar spine
6% dense
59 year old male

Ralph Muller, ETH Zurich
Micro-CT images

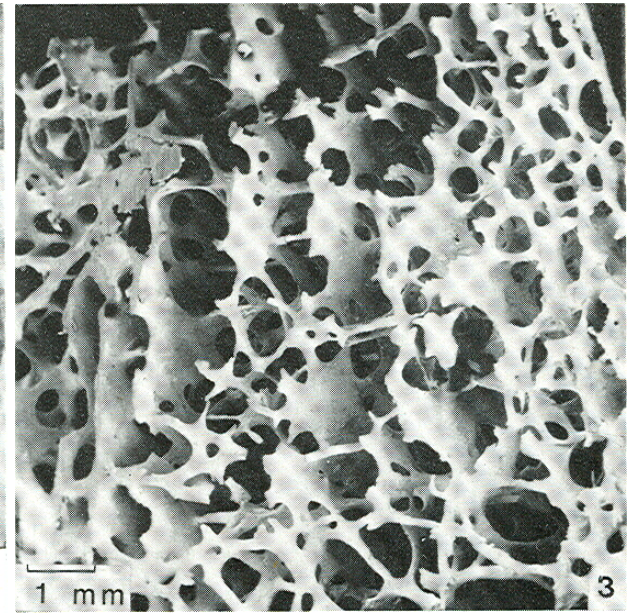
Trabecular Bone Structure



Femoral head



Femoral head



Femoral condyle (knee)

Source: Gibson, L. J. "[The Mechanical Behaviour of Cancellous Bone](#)." *Journal of Biomechanics* 18 (1985): 317-28. Courtesy of Elsevier. Used with permission.

Bone grows with response to loads

- Studies on juvenile guinea fowl (Ponzer et al 2006)
 - (a) running on level treadmill
 - (b) running on inclined treadmill (20°)
 - (c) control — no running
- Measured knee flexion angle at max force on treadmill
- After ~ 6 weeks, sacrificed birds and measured orientation of peak trabecular density (OPTD)
- Knee flexion angle changed by 13.7° with incline vs level treadmill running
- OPTD changed by 13.6° with incline vs level treadmill running
- Orientation of trabecula changed to match orientation of loading
- Video: Concord Field Station (Science Friday)

Trabecular architecture and mechanical loading

Figure removed due to copyright restrictions. See Figure 1: Pontzer, H., et al. "[Trabecular Bone in the Bird Knee Responds with High Sensitivity to Changes in Load Orientation.](#)" *The Journal of Experimental Biology* 209 (2006): 57-65.

Trabecular architecture and mechanical loading

Figure removed due to copyright restrictions. See Figure 7: Pontzer, H., et al. "[Trabecular Bone in the Bird Knee Responds with High Sensitivity to Changes in Load Orientation.](#)" *The Journal of Experimental Biology* 209 (2006): 57-65.

Video: "[Studying Locomotion With Rat Treadmills, Wind Tunnels.](#)" March 9, 2012. Science Friday. Accessed November 12, 2014.

Properties of solid in trabeculae

- Foam models: require ρ_s , E_s , σ_{ys} for the solid
- Ultrasonic wave propagation $E_s = 15 - 18$ GPa
- Finite element models of exact trabecular architecture from micro-CT scans
If do uniaxial compression test — can measure E^* and back-calculate E_s
 $E_s = 18$ GPa
- Find properties of trabeculae (solid) similar to cortical bone:

$$\rho_s = 1800 \text{ kg/m}^3$$

$$E_s = 18 \text{ GPa}$$

$$\sigma_{ys} = 182 \text{ MPa (compression)}$$

$$\sigma_{ys} = 115 \text{ MPa (tension)}$$

Mechanical Properties of Trabecular Bone

- Compressive stress-strain curve - characteristic shape
- Mechanisms of deformation and failure
 - Usually bending followed by inelastic buckling
 - Sometimes, if trabeculae are aligned or very dense: axial deformation
 - Observations by deformation stage in μCT ; also FEA modeling
- Tensile $\sigma - \epsilon$ curve: failure at smaller strains; trabecular micro cracking
- Data for E^* , σ_c^* , σ_T^* (normalized by values for cortical bone)
 - Spread is large — anisotropy, alignment of trabecular orientation and loading direction; variations in solid properties, $\dot{\epsilon}$, species
- Models — based on open-cell foams

Compression $E^*/E_s \propto (\rho^*/\rho_s)^2$ bending
 $\sigma_{el}^*/E_s \propto (\rho^*/\rho_s)^2$ buckling
 Tension $\sigma_T^*/\sigma_{ys} \propto (\rho^*/\rho_s)^{3/2}$ plastic hinges

Data generally consistent
 with models
 Also: statistical analysis of data
 $E^*, \sigma_c^* \propto \rho^2$

Note: compression: $\epsilon_{el}^* = \text{constant} = 0.7\%$

Compressive stress-strain curves

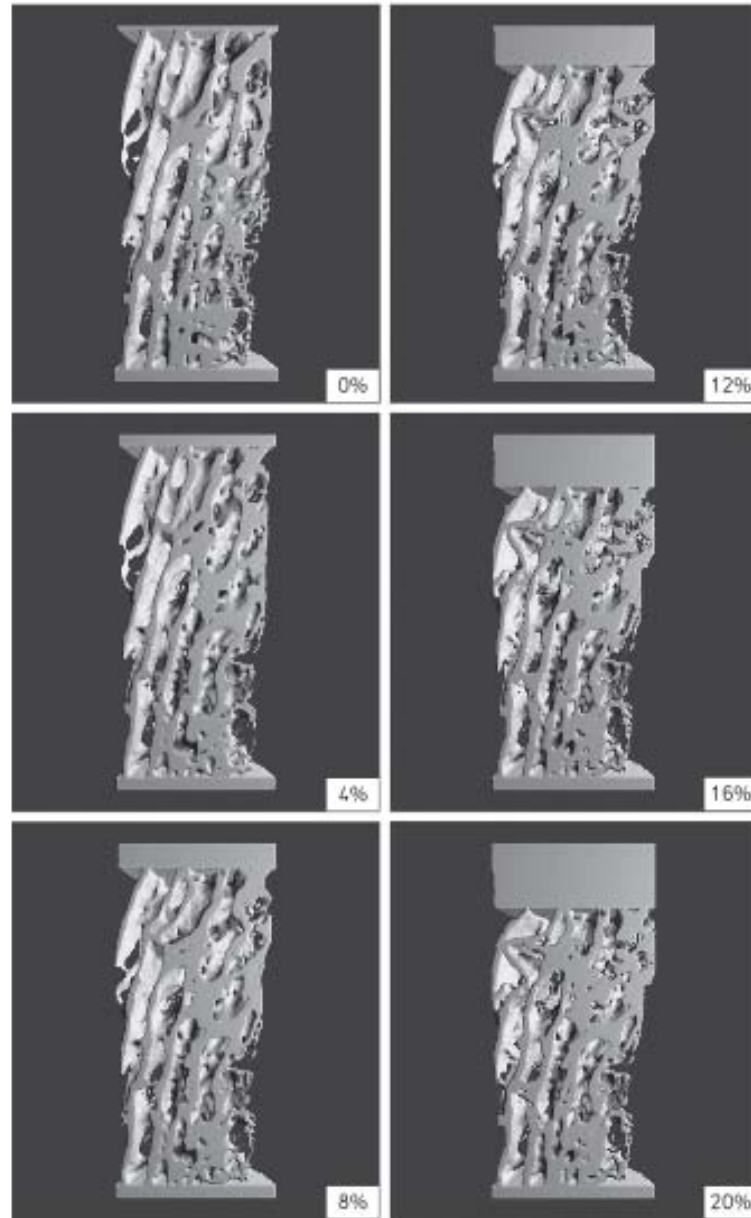
Figure removed due to copyright restrictions. See Fig. 1: Hayes, W. C., and D. R. Carter. "[Postyield Behavior of Subchondral Trabecular Bone](#)." *Journal of Biomedical Materials Research* 10, no. 4 (1976): 537-44.

Hayes and Carter, 1976

Compression Whale Vertebra

Images removed due to copyright restrictions. See Figure 5: Müller, R. S. C. Gerber, and W. C. Hayes. "[Micro-compression: A Novel Technique for the Non-destructive Assessment of Bone Failure](#)." *Technology and Health Care* 6 (1998): 433-44.

Muller et al, 1998



Nazarian and Muller 2004

Source: Narzarian, A., and R. Müller. "Time-lapsed Microstructural Imaging of Bone Failure Behavior." *Journal of Biomechanics* 37 (2000): 1575-83. Courtesy of Elsevier. Used with permission.

Images removed due to copyright restrictions.

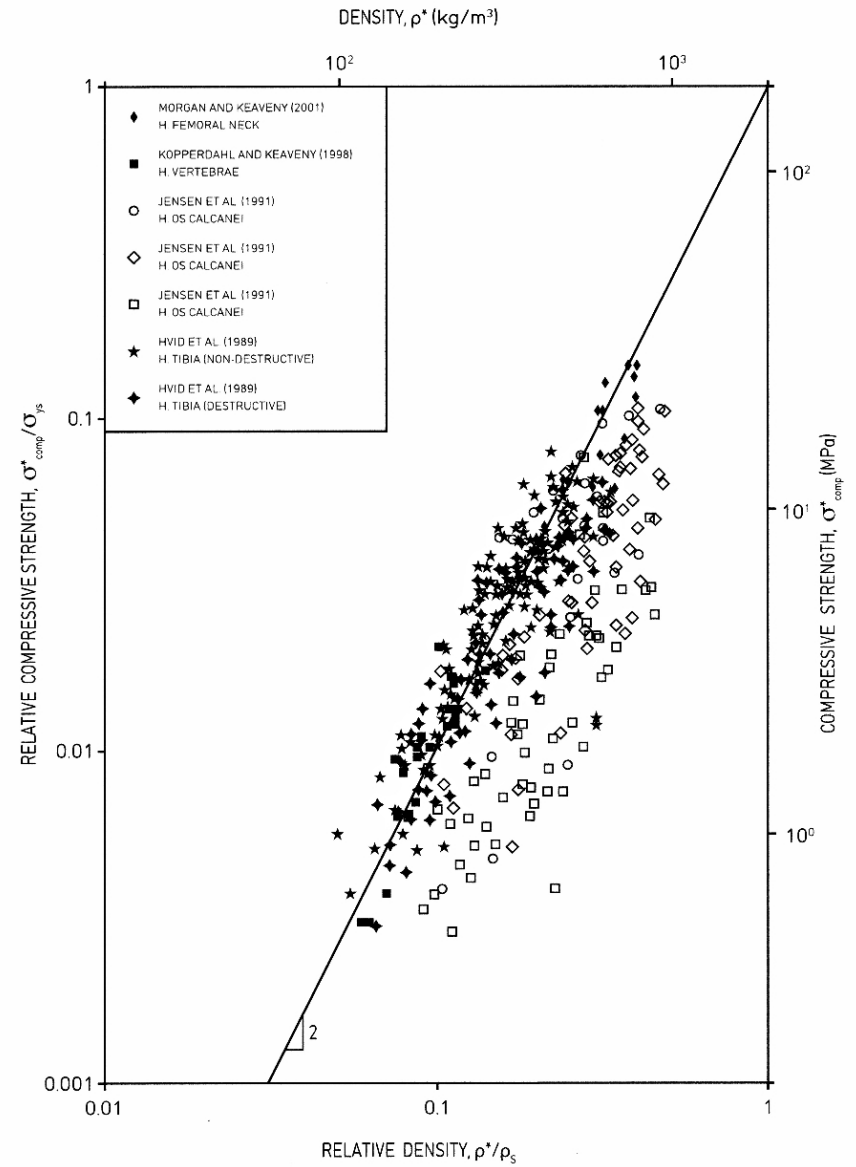
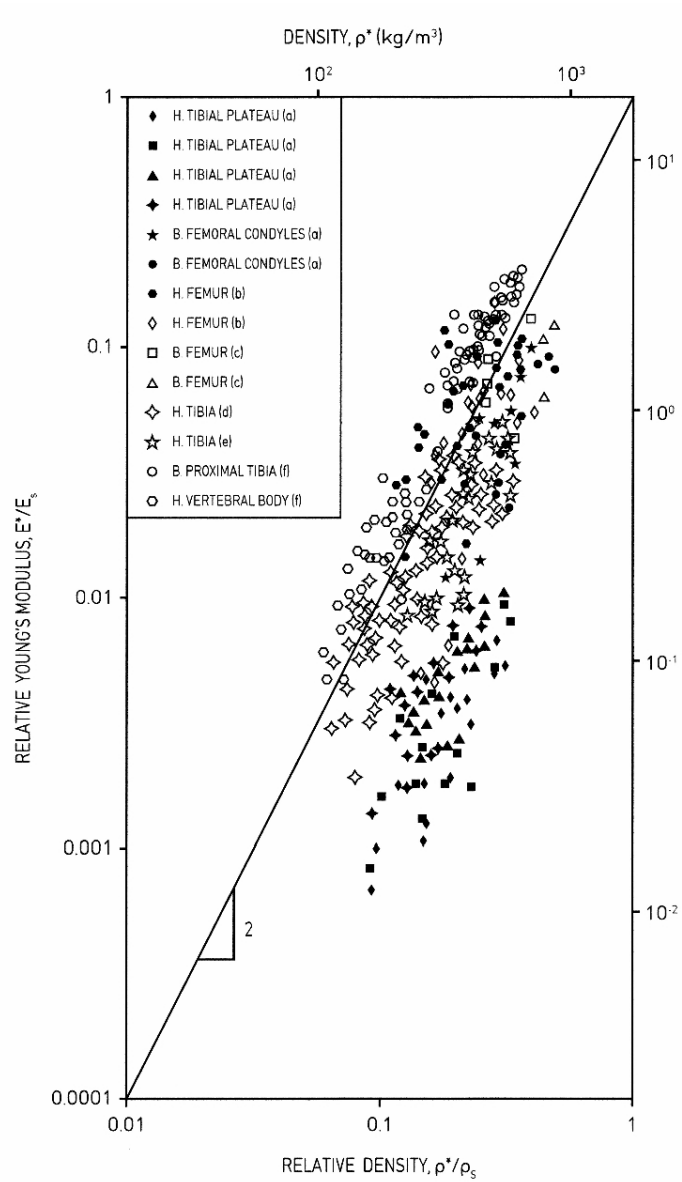
Human Vertebral Bone

Mueller, ETH

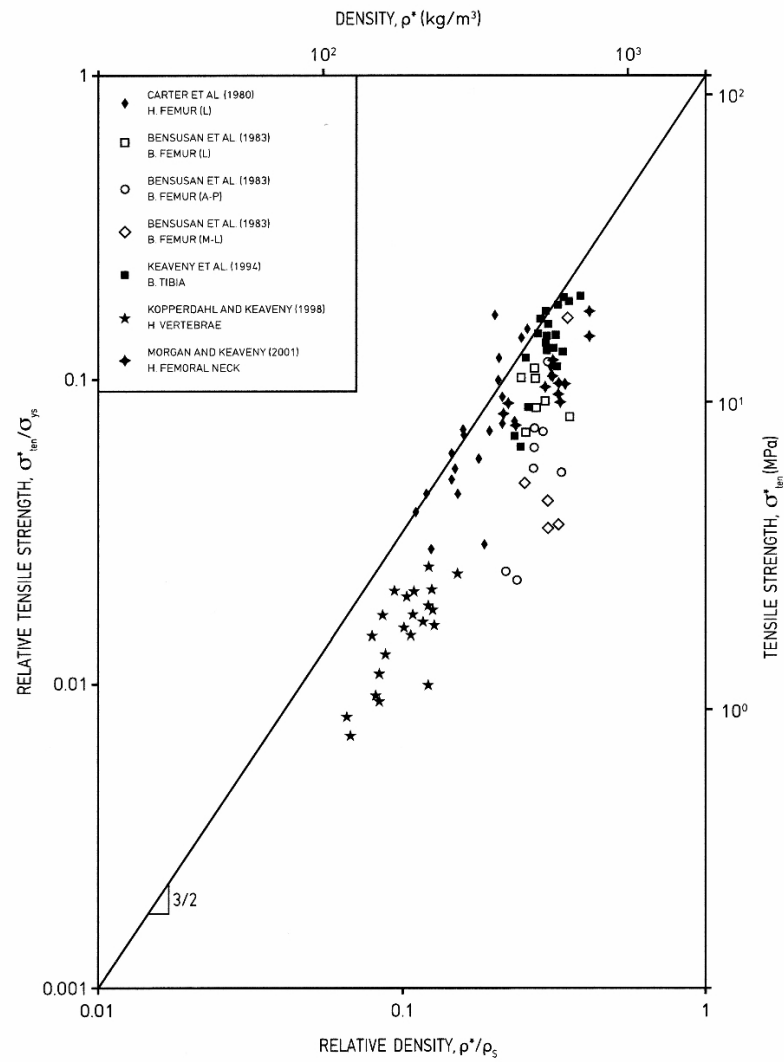
Tension

Figure removed due to copyright restrictions. See Fig. 5.6: Gibson, L. J., et al. *Cellular Materials in Nature and Medicine*. Cambridge University Press, 2010.

Carter et al., 1980



Gibson, L. J., M. Ashby, et al. *Cellular Materials in Nature and Medicine*. Cambridge University Press, © 2010. Figures courtesy of Lorna Gibson and Cambridge University Press.



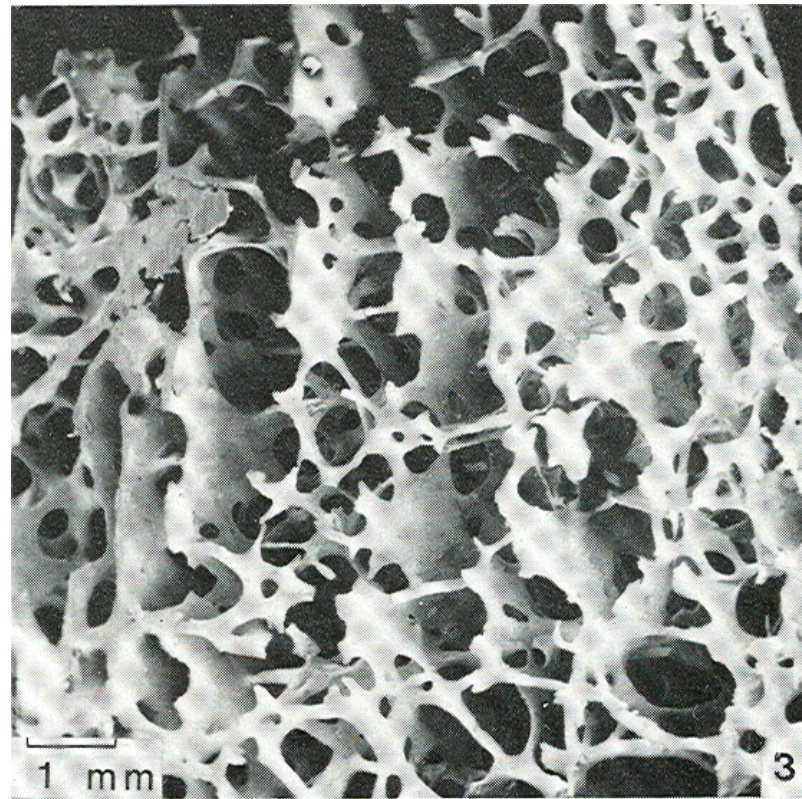
Gibson, L. J., M. Ashby, et al. *Cellular Materials in Nature and Medicine*. Cambridge University Press, © 2010. Figure courtesy of Lorna Gibson and Cambridge University Press.

- In some regions, trab. may be aligned: e.g. parallel plates
 - deformation then axial $E^* \propto \rho$
(in longitudinal direction) $\sigma^* \propto \rho$
- Can also summarize data for solid trabeculae and trabecular bone (similar to wood)
Solid-composite of hydroxyapatite and collagen

Osteoporosis (Latin: “porpus bones”)

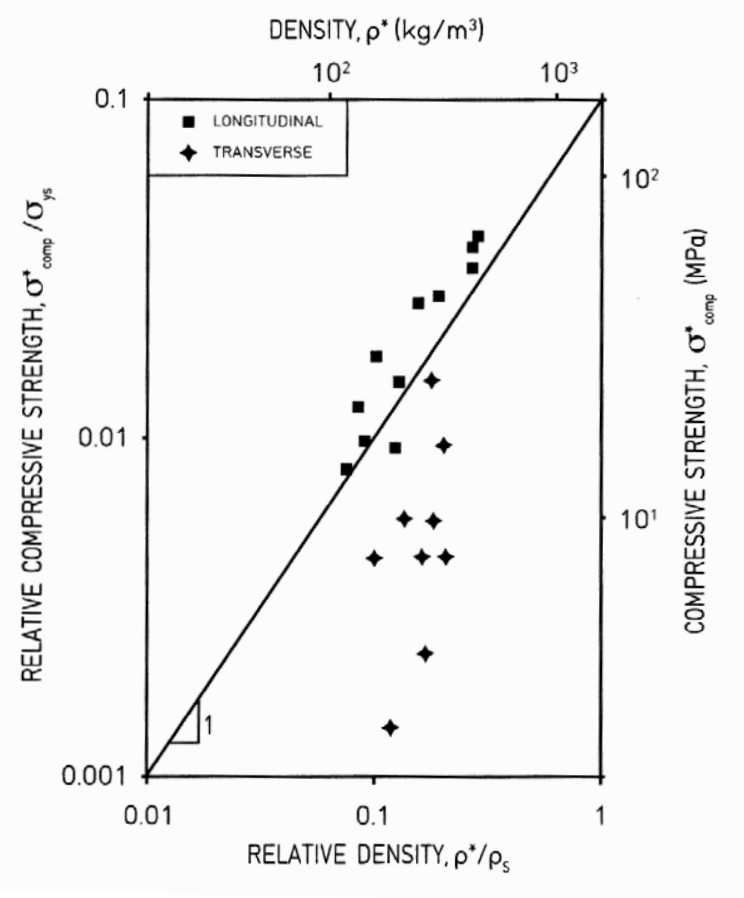
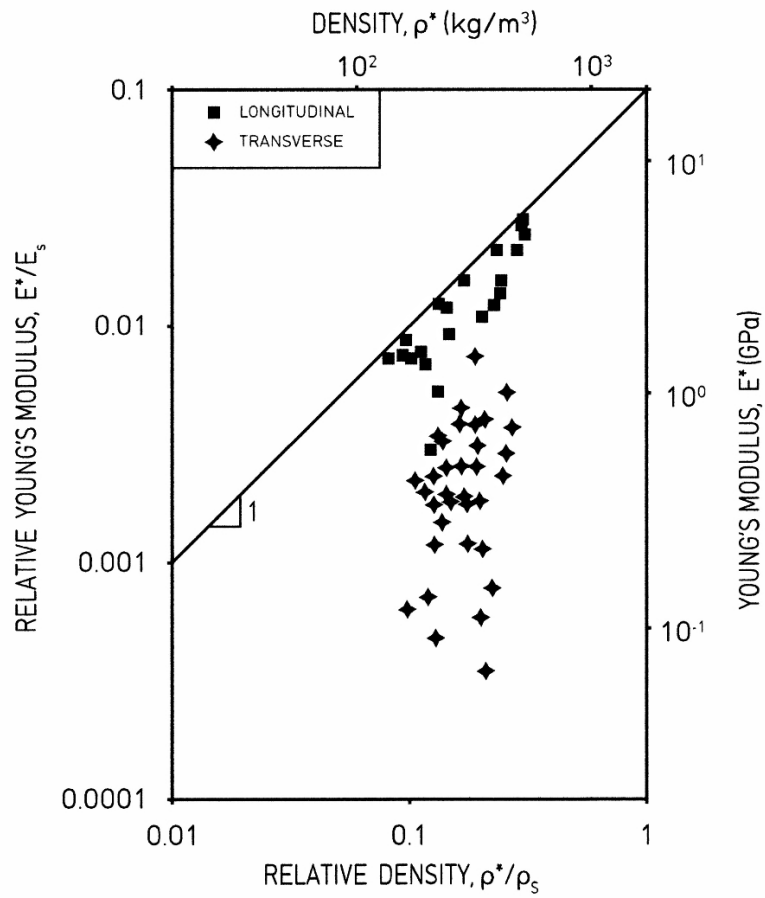
- As age, lose bone mass
- Bone mass peaks at 25 years, then decreases 1-2% per year
- Women, menopause — cessation of estrogen production, increases rate of bone loss
- Osteoporosis defined as bone mass 2.5 standard deviations (or more) below young normal mean
- Trabeculae thin and then resorb completely

Aligned Trabeculae

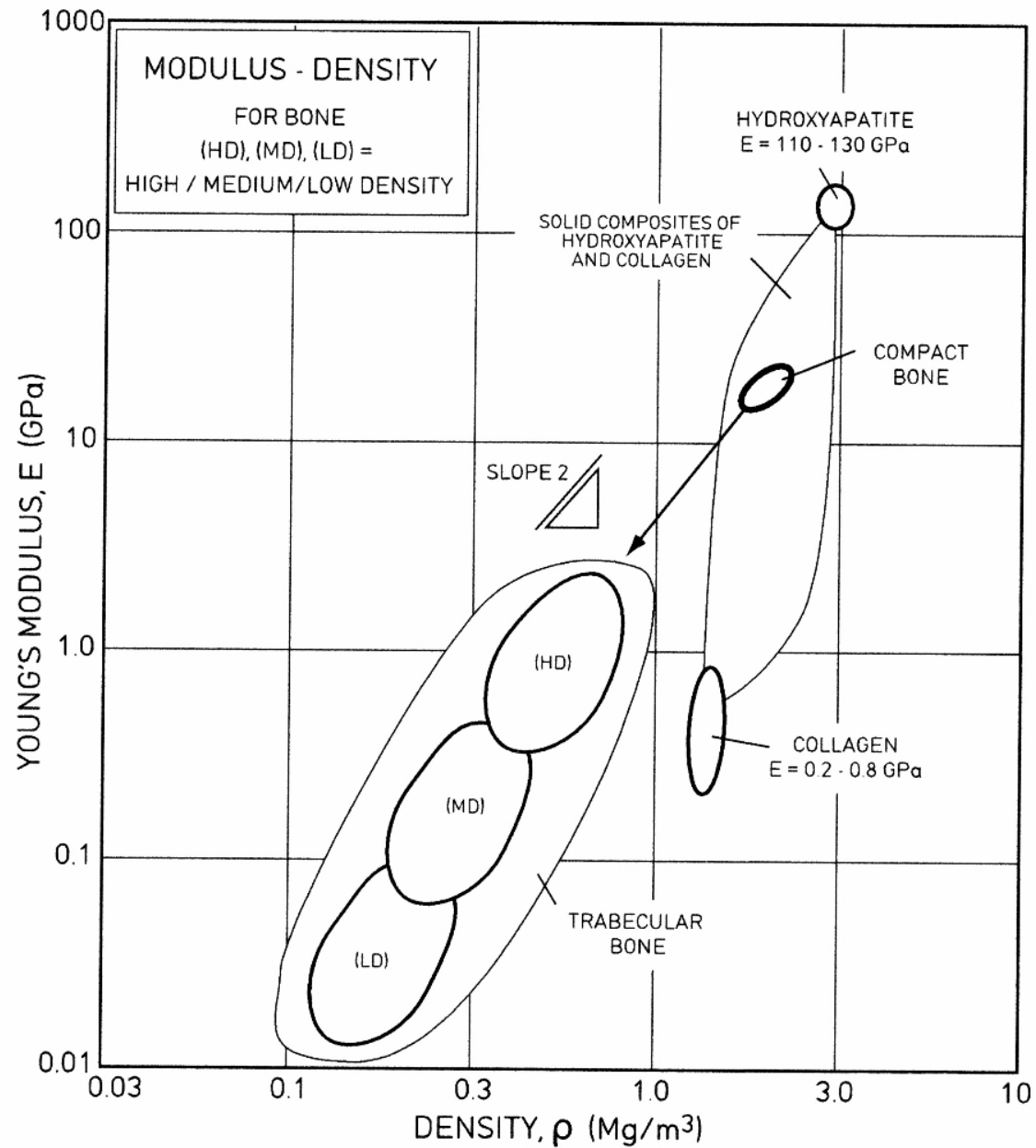


Femoral Condyle (Knee)

Source: Gibson, L. J. "The Mechanical Behaviour of Cancellous Bone." *Journal of Biomechanics* 18 (1985): 317-28. Courtesy of Elsevier. Used with permission.



Gibson, L. J., M. Ashby, et al. *Cellular Materials in Nature and Medicine*. Cambridge University Press, © 2010. Figures courtesy of Lorna Gibson and Cambridge University Press.



Gibson, L. J., M. Ashby, et al. *Cellular Materials in Nature and Medicine*. Cambridge University Press, © 2010. Figure courtesy of Lorna Gibson and Cambridge University Press.

Osteoporosis

Figure removed due to copyright restrictions. See Figure 1: Vajjhala, S., A. M. Kraynik, et al. "[A Cellular Solid Model for Modulus Reduction due to Resorption of Trabecular Bone.](#)" *Journal of Biomechanical Engineering* 122, no. 5 (2000): 511–15.

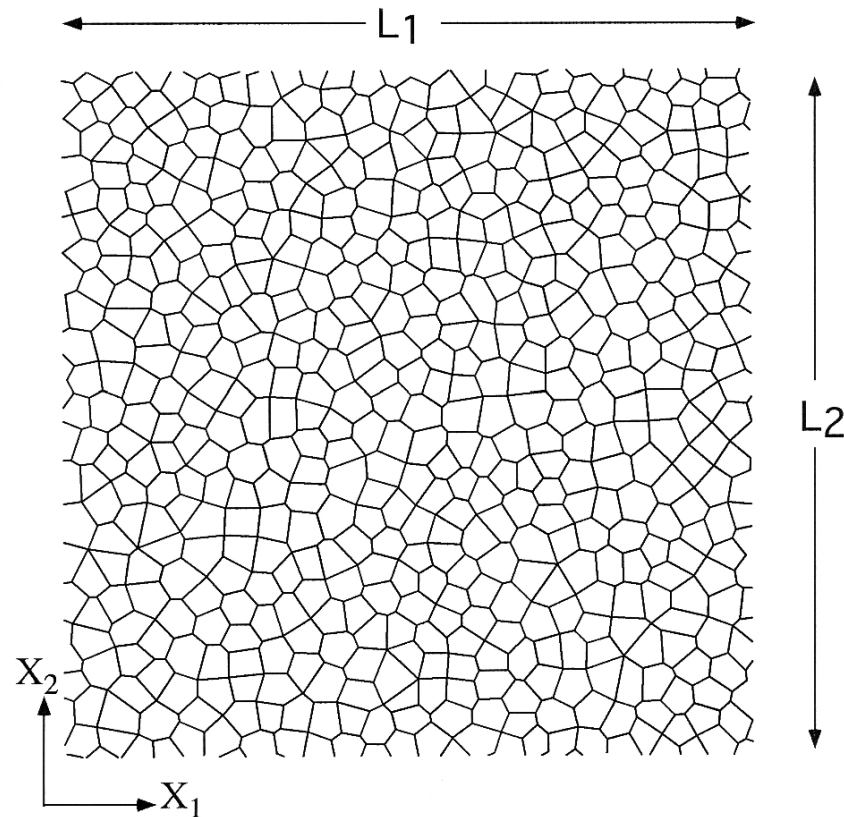
- As trabeculae thin - buckling easier $\sigma^* \propto (\rho/\rho_s)^2$
- Once trabeculae begin to resorb, connectivity reduced, strength drops dramatically
- Modeling:
 - Can't use unit cell or dimensional analysis (need to model local effects)
 - Finite element modeling
 - Initially:
 - 2D Voronoi honeycombs
 - 2D representation of vertebral bone
 - 3D Voronoi foam — Surekha Vajjbala

} Matt Silva

Voronoi honeycomb

- Random seed points, draw perpendicular bisectors
- Use a minimum separation distance to get cells of approximately uniform size
- FE analysis — each trabecula a beam element
- First calculated elastic moduli
 - FEA results close to analytical model for random (isotropic) honeycomb (40 models, all same ρ^*/ρ_s , about 25x25 cells in each)
 - Modulus is average of stiffness over entire material

Modelling: 2D Voronoi

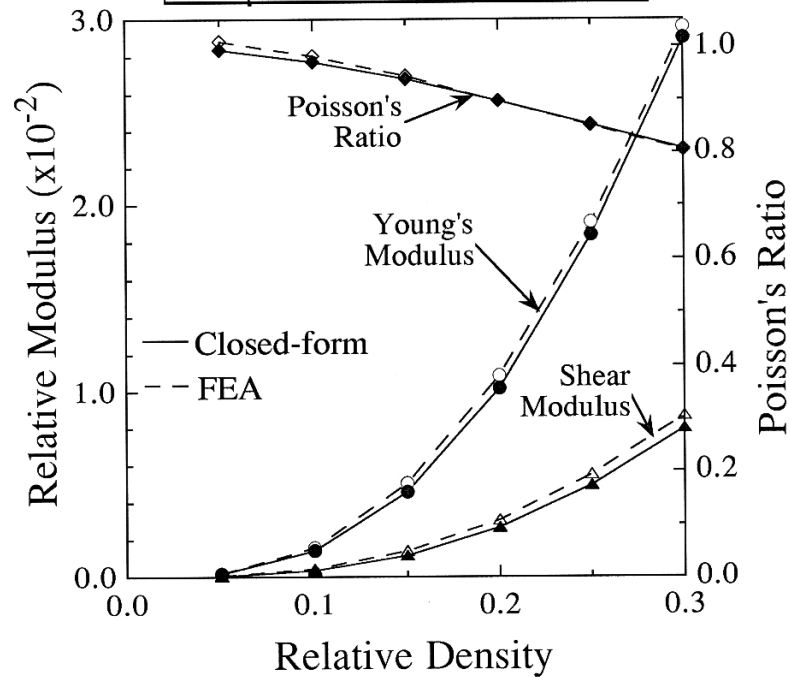


Silva et al, 1995

Source: Silva, M. J., L. J. Gibston, et al. "The Effects of Non-periodic Microstructure on the Elastic Properties of Two-dimensional Cellular Solids." *International Journal of Mechanical Sciences* 37 (1995): 1161-77. Courtesy of Elsevier. Used with permission.

2D Voronoi

E^*/E_s	FEA	$y=0.56x^{2.43}$
E^*/E_s	Equation (1a)	$y=0.63x^{2.54}$
G^*/E_s	FEA	$y=0.18x^{2.53}$
G^*/E_s	Equation (3d)	$y=0.20x^{2.68}$
ν^*	FEA	$y= -1.20x^{1.38} + 1.0$
ν^*	Equation (1b)	$y= -1.30x^{1.55} + 1.0$



Silva et al, 1995

Source: Silva, M. J., L. J. Gibston, et al. "The Effects of Non-periodic Microstructure on the Elastic Properties of Two-dimensional Cellular Solids." *International Journal of Mechanical Sciences* 37 (1995): 1161-77. Courtesy of Elsevier. Used with permission.

- Next, calculated compressive strength of Voroni honeycombs
- Each cell wall 1-3 beam elements
- Model non-linear elasticity and failure behavior
- 15x15 cells in model (random seeds \approx isotropic)
- Cell wall assumed to be elastic – perfectly plastic $\sigma_{ys}/E_s = 0.01$ $v_s = 0.3$
- For this value of σ_{ys}/E_s , transition between elastic buckling and plastic collapse stress at $\rho^*/\rho_s = 0.035$ in regular hexagonal honeycomb
- Calculated compressive strength of honeycombs with $\rho^*/\rho_s = 0.015, 0.035, 0.05, 0.15$
- Generated 5 different Voronoi honeycombs at each ρ^*/ρ_s
- Compressive $\sigma - \epsilon$ behavior:

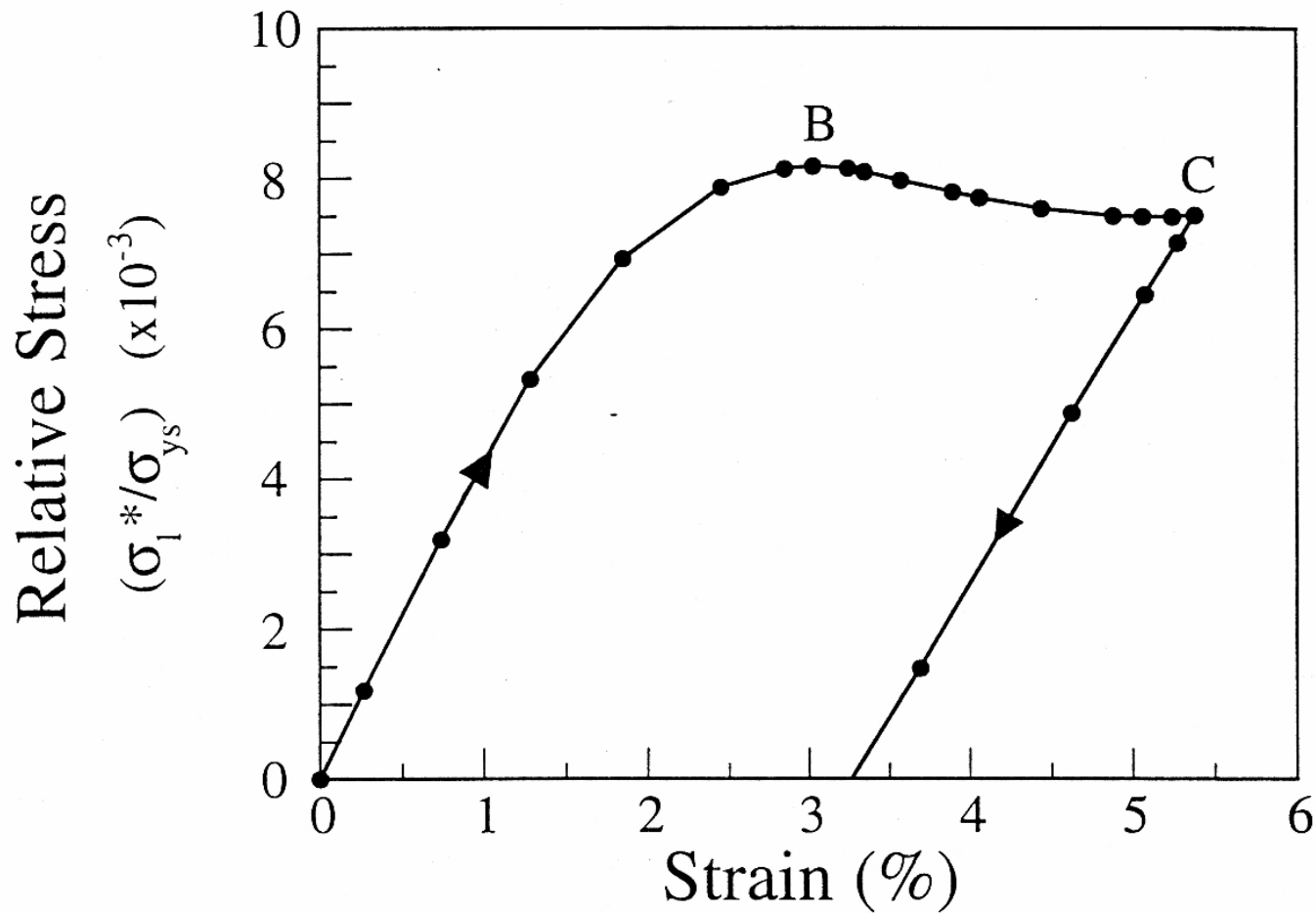
$\rho^*/\rho_s \geq 0.05$ -strain softening, permanent deformation on unloading

-plastic hinge formation, cell collapse in narrow localized bands

$\rho^*/\rho_s < 0.035$ -non-linear elastic deformation - recoverable

Strength: 0.6 to 0.8 of $\sigma_{\text{periodic}}^*$

2D Voronoi

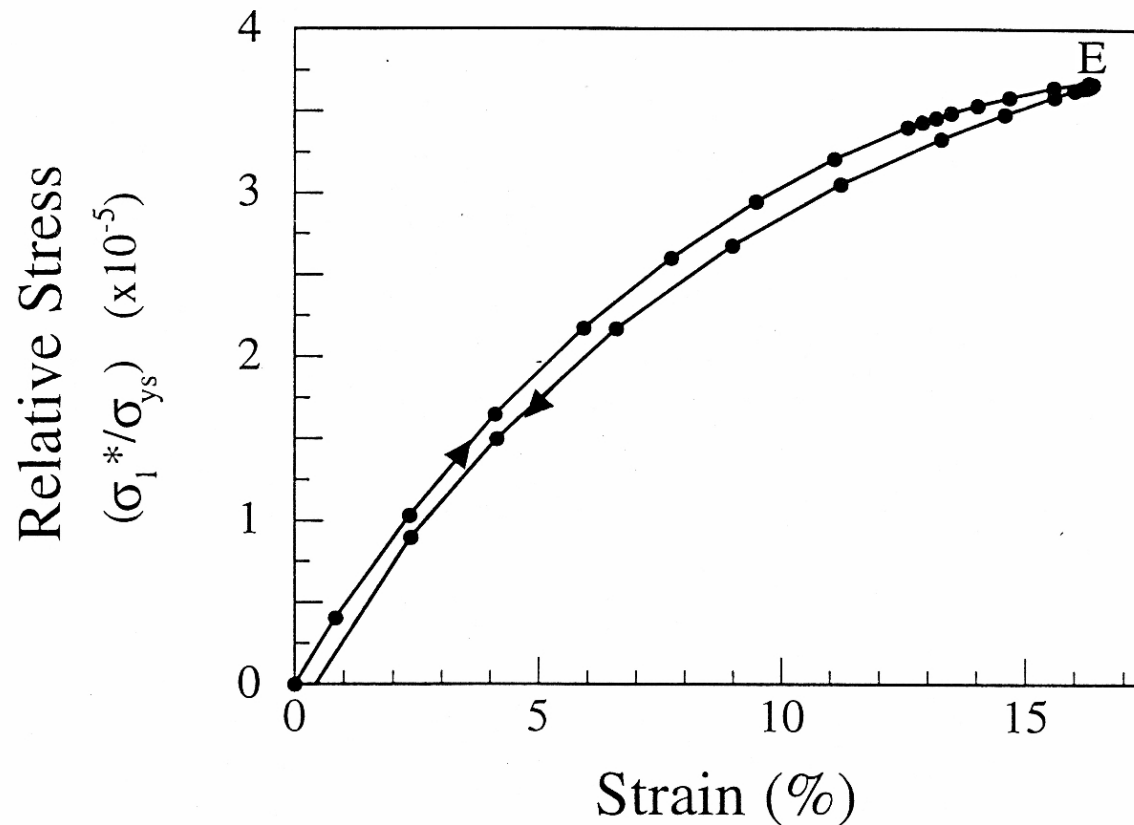


Relative density = 15% Plastic failure

Silva et al, 1997

Source: Silva, M. J., and L. J. Gibson. "The Effects of Non-periodic Microstructure and Defects on the Compressive Strength of Two-dimensional Cellular Solids." *International Journal of Mechanical Sciences* 39 (1997b): 549-63. Courtesy of Elsevier. Used with permission.

2D Voronoi

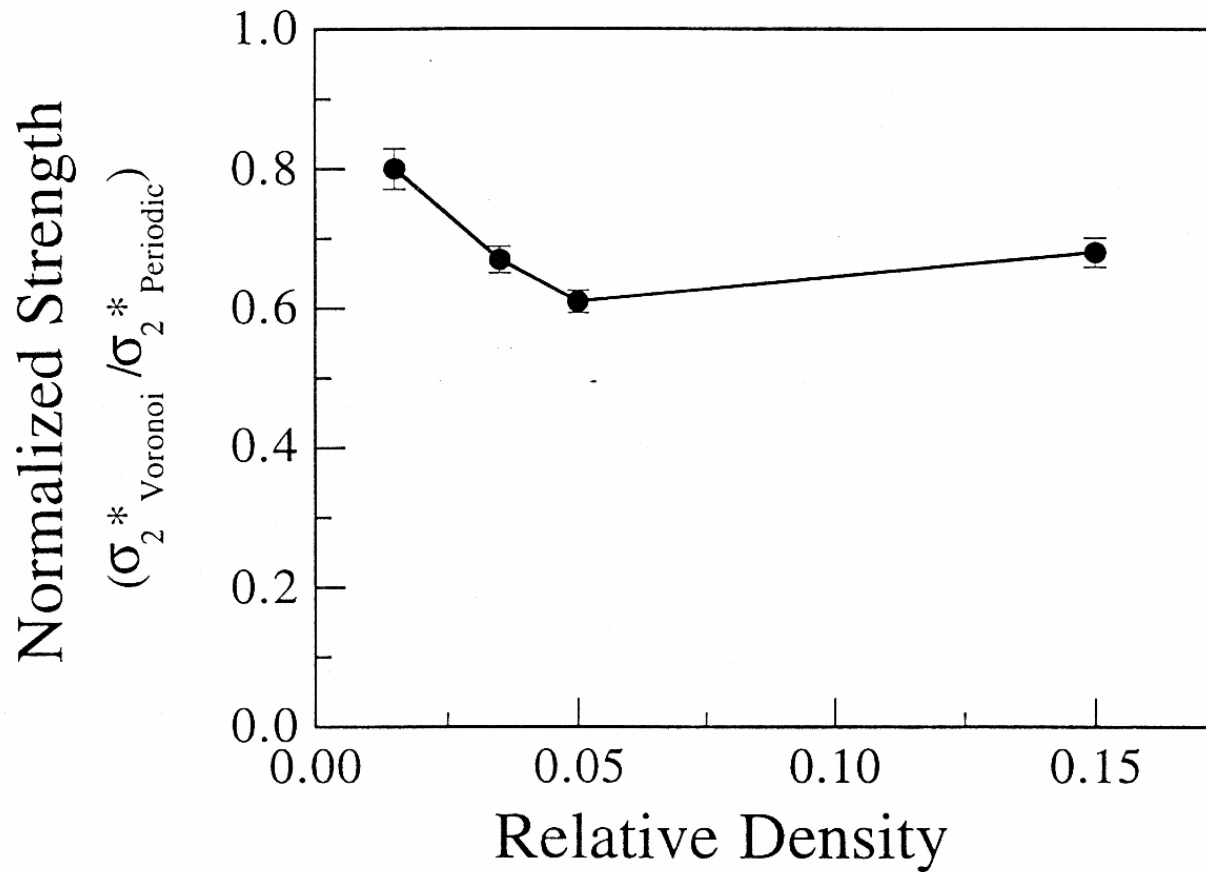


Relative density 1.5%; elastic buckling failure

Silva et al, 1997

Source: Silva, M. J., and L. J. Gibson. "The Effects of Non-periodic Microstructure and Defects on the Compressive Strength of Two-dimensional Cellular Solids." *International Journal of Mechanical Sciences* 39 (1997b): 549-63. Courtesy of Elsevier. Used with permission.

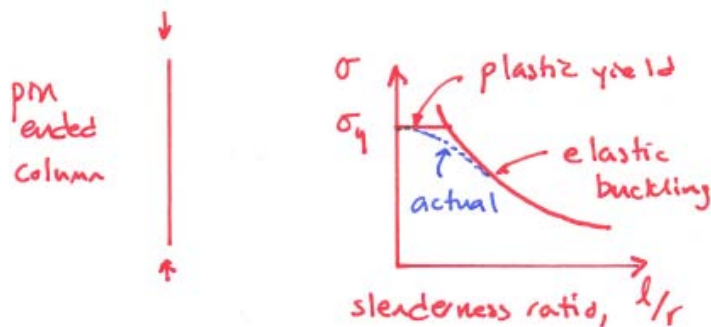
2D Voronoi



Silva et al, 1997

Source: Silva, M. J., and L. J. Gibson. "The Effects of Non-periodic Microstructure and Defects on the Compressive Strength of Two-dimensional Cellular Solids." *International Journal of Mechanical Sciences* 39 (1997b): 549-63. Courtesy of Elsevier. Used with permission.

- Max. normal strains at nodes in honeycombs (linear elastic).
 - Voronoi honeycombs — normal distribution
 - Regular hexagonal honeycombs — dashed lines on plot
 - Normal strain in vertical cell walls in regular hexagonal honeycombs — mean normal strain in Voronoi
 - Oblique walls — bending — larger strains
 - Voronoi honeycomb 5% of strain outside of range of strain in regular hexagonal honeycomb
 - Decrease in strength associated with broader range of strains in Voronoi honeycombs
 - Minimum strength at $\rho^*/\rho_s = 0.05$
 - Interaction between elastic buckling and plastic yield



$$\sigma_{cr} = \frac{\pi^2 EI}{l^2} = \frac{\pi^2 E \pi r^4}{4 l^2 \pi r^2} = \frac{\pi^2}{4} E \left(\frac{r}{l}\right)^2$$

2D Voronoi

Figure removed due to copyright restrictions. See Figure 5; Silva, M. J., and L. J. Gibson. "[The Effects of Non-periodic Microstructure and Defects on the Compressive Strength of Two-dimensional Cellular Solids.](#)" *International Journal Mechanical Sciences* 39, no. 5 (1997): 549-63.

Silva et al, 1997

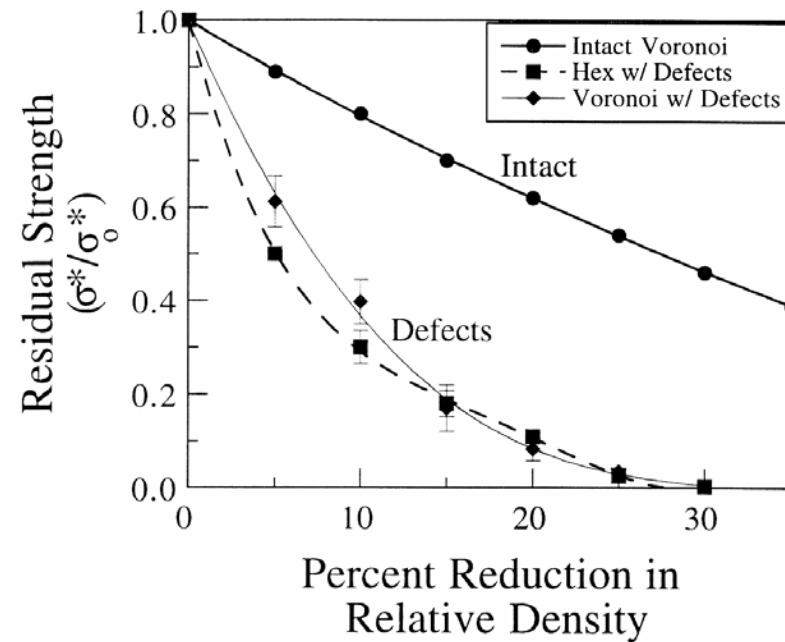
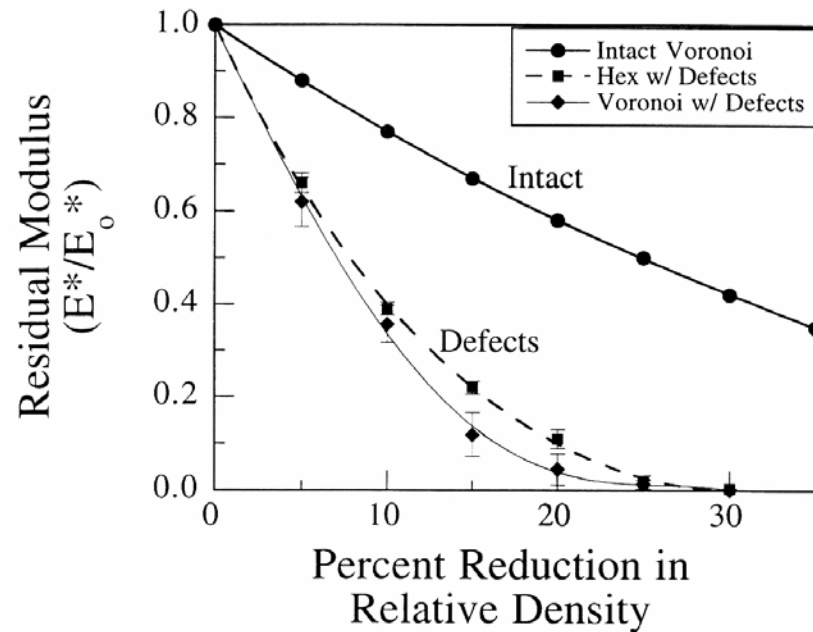
Voronoi honeycombs - defects

- Randomly removed cell walls in both Voronoi and regular honeycombs
- Analyzed both by FEA
- Dramatic decrease in modulus and strength, compared with equivalent reduction in density by thinning of cell walls
- $\rho^*/\rho_s = 0.15$ failure by yielding
- $\rho^*/\rho_s = 0.015$ failure by elastic buckling
- Modulus and strength reduction similar for Voronoi and regular hexagonal honeycombs
- Percolation threshold for $2D$ network hexagonal cells \Rightarrow 35% struts removed

Vertebral trabecular bone - 2D model

- Model adapted to reflect trabeculae more aligned in vertical and horizontal directions
- Perturbed a square array of struts to get similar orientation and struts as in bone
- Looked at reduction in number and thickness of longitudinal and transverse struts (independently)

2D Voronoi



Source: Silva, M. J., and L. J. Gibson. "The Effects of Non-periodic Microstructure and Defects on the Compressive Strength of Two-dimensional Cellular Solids." *International Journal of Mechanical Sciences* 39 (1997b): 549-63. Courtesy of Elsevier. Used with permission.

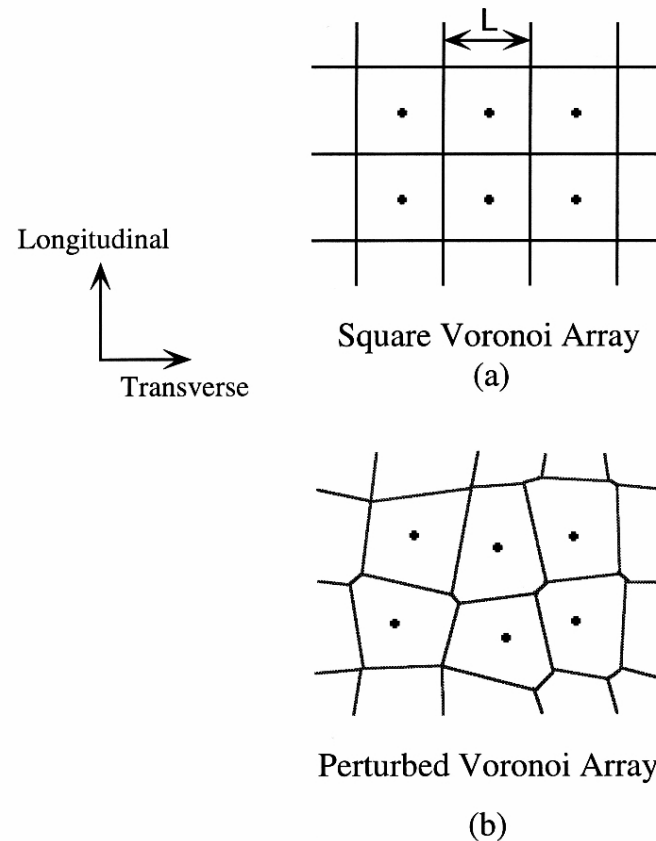
Silva et al, 1997

2D Voronoi

Figure removed due to copyright restrictions. See Figure 2: Vajjhala, S., A. M. Kraynik, et al. "[A Cellular Solid Model for Modulus Reduction due to Resorption of Trabecular Bone.](#)" *Journal of Biomechanical Engineering* 122, no. 5 (2000): 511–15.

Vajjhala et al, 2000

Vertebral Trabecular Bone



Source: Silva, M. J., and L. J. Gibson. "Modelling the Mechanical Behavior of Vertebral Trabecular Bone: Effects of Age-related Changes in Microstructure." *Bone* 21 (1997a): 191-99. Courtesy of Elsevier. Used with permission.

Silva et al, 1997

Vertebral Trabecular Bone

Figure removed due to copyright restrictions. See Figure 3: Silva, M. J., and L. J. Gibson. "[Modelling the Mechanical Behavior of Vertebral Trabecular Bone: Effects of Age-related Changes in Microstructure.](#)" *Bone* 21 (1997): 191-99.

Silva et al, 1997

Vertebral Trabecular Bone

Figure removed due to copyright restrictions. See Figure 4: Silva, M. J., and L. J. Gibson. "[Modelling the Mechanical Behavior of Vertebral Trabecular Bone: Effects of Age-related Changes in Microstructure](#)." *Bone* 21 (1997): 191-99.

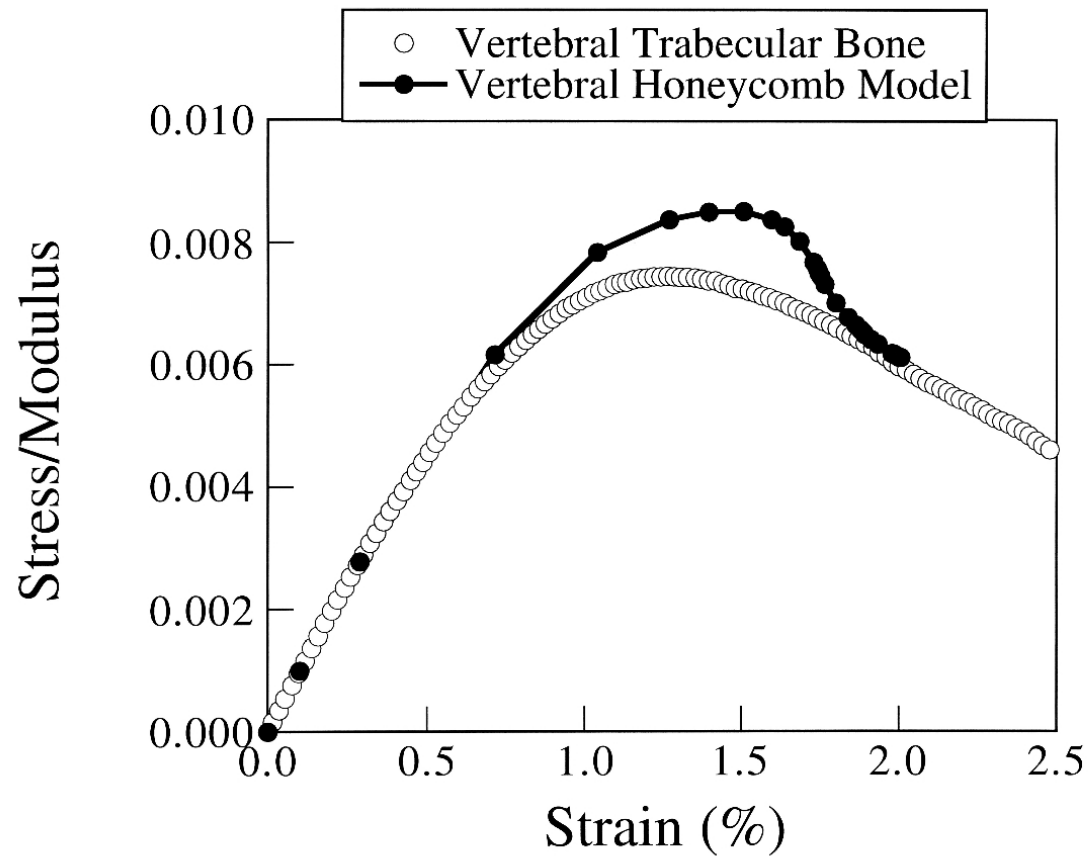
Silva et al, 1997

Vertebral Trabecular Bone

Figure removed due to copyright restrictions. See Figure 5: Silva, M. J., and L. J. Gibson. "[Modelling the Mechanical Behavior of Vertebral Trabecular Bone: Effects of Age-related Changes in Microstructure](#)." *Bone* 21 (1997): 191-99.

Silva et al, 1997

Vertebral Trabecular Bone



Source: Silva, M. J., and L. J. Gibson. "Modelling the Mechanical Behavior of Vertebral Trabecular Bone: Effects of Age-related Changes in Microstructure." *Bone* 21 (1997a): 191-99. Courtesy of Elsevier. Used with permission.

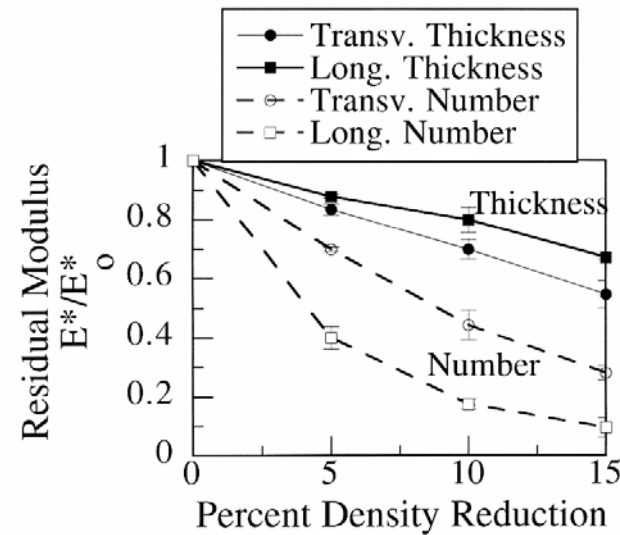
Silva et al, 1997

Vertebral Trabecular Bone

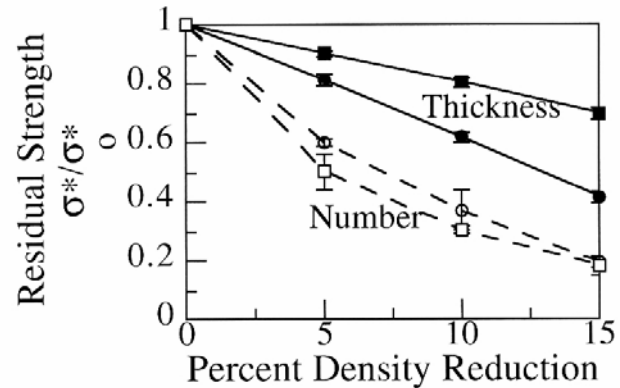
Figure removed due to copyright restrictions. See Figure 7: Silva, M. J., and L. J. Gibson. "[Modelling the Mechanical Behavior of Vertebral Trabecular Bone: Effects of Age-related Changes in Microstructure](#)." *Bone* 21 (1997): 191-99.

Silva et al, 1997

Vertebral Trabecular Bone



(a)



(b)

Silva et al, 1997

Source: Silva, M. J., and L. J. Gibson. "Modelling the Mechanical Behavior of Vertebral Trabecular Bone: Effects of Age-related Changes in Microstructure." *Bone* 21 (1997a): 191-99. Courtesy of Elsevier. Used with permission.

3D Voronoi Model

- Same analysis, now with 3D Voronoi model
- Periodic 3x3x3 cells, $\rho^*/\rho_s = 0.1$
- Used beam elements, FEA, linear elastic only
- Percolation threshold $\sim 50\%$ struts removed
- Comparison of 2D and 3D results for modulus: in 3D, modulus reduction more gradual than in 2D
- Also for 2D and 3D — modulus reduction similar for regular and Voronoi structures

3D Voronoi Model

Figure removed due to copyright restrictions. See Figure 7: Vajjhala, S., A. M. Kraynik, et al. "[A Cellular Solid Model for Modulus Reduction due to Resorption of Trabecular Bone.](#)" *Journal of Biomechanical Engineering* 122, no. 5 (2000): 511–15.

Vajjhala et al, 2000

3D Voronoi Model

Figure removed due to copyright restrictions. See Figure 7: Vajjhala, S., A. M. Kraynik, et al. "[A Cellular Solid Model for Modulus Reduction due to Resorption of Trabecular Bone.](#)" *Journal of Biomechanical Engineering* 122, no. 5 (2000): 511–15.

Vajjhala et al, 2000

Metal foams as bone substitute materials

- Metals used in orthopedic implants (e.g. hip, knee)
- Co-Cr, Ti, Ta, stainless steel alloys
- Biocompatible, corrosion resistant
- But moduli of metals are greater than modulus of bone
e.g. $E_{Ti} = 110 \text{ GPa}$, $E_{cortical} = 18 \text{ GPa}$, $E_{trab.bone} = 0.01 - 2 \text{ GPa}$
- Stress shielding can lead to bone resorption
- To improve mechanical interaction between implant and bone:
 - porous sintered metal beads used to coat implants - promote bone ingrowth
 - also, wire mesh coatings have been developed, primarily for flat implant surfaces
 - recently, interest in using metal foams as coatings
 - longer term, interest in using in replacement vertebral bodies
- Variety of processes for making metal foam implant coatings

Metal Foams: Microstructure

Ta, replicating PU foam
with CVD

Ti, replication of PU
foam by slurry infiltration
and sintering

Ti, fugitive phase

Ti, foaming agent

Ti, expansion of Ar gas

Images removed due to copyright restrictions. See Figure 8.1:
Gibson, L. J., M. Ashby, and B. A. Harley. *Cellular Materials in
Nature and Medicine*. Cambridge University Press, 2010.
<http://books.google.com/books?id=AKxiS4AKpyEC&pg=PA228>

Ti, freeze-casting
(freeze-drying)

Ti, selective laser
sintering

Ni-Ti, high temperature
synthesis (powders
mixed, pressed and
ignited by, for example,
tungsten coil heated by
electrical current)

Image sources given in
*Cellular Materials in Nature
and Medicine*

Processing

(a) Replicate open cell polyurethane foam

- Pyrolyze PU foam \rightarrow 2% dense vitreous carbon
- Coat with Ta by CVD \Rightarrow struts 99% Ta, 1% C
- Cell size 400 – 600 μm ; coating thickness 40 – 60 μm , $\rho^*/\rho_s = 0.15 - 0.25$
- “Trabecular metal” (Zimmer) trade name
- Ta forms surface oxide Ta_2O_5 — does not bond to bone
- But, if treat with dilute NaOH, then heat to 300°C and cool, then submerge in simulated body fluid (ion concentration matches human blood plasma)
 \Rightarrow get apatite coating on foam struts, which bonds to bone

(b) Infiltrate slurry of titanium hydride into open cell foam

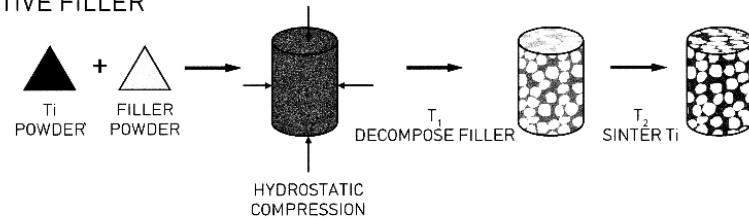
- Heat-treat to decompose TiH_2
- Sinter remaining Ti (also removes initial foam)

(c) Fugitive phase methods

- Mix Ti powder and fugitive phase powder
- Heat to T_1 ($\sim 200^\circ\text{C}$) to decompose filler, then to T_2 (1200°C) to sinter Ti powder

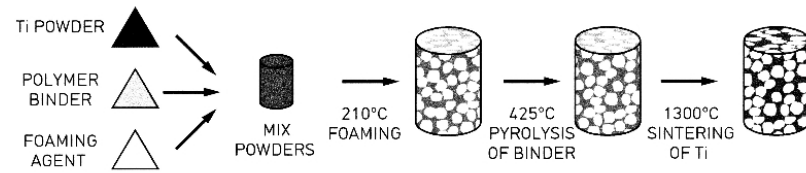
Metal Foams: Processing

FUGITIVE FILLER



(a)

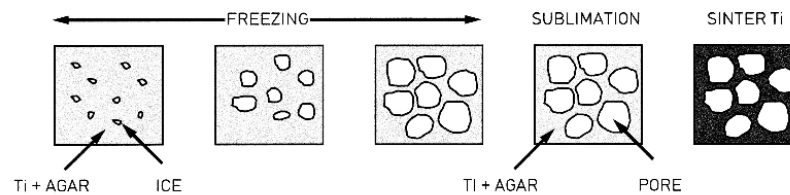
EXPANSION OF A FOAMING AGENT



Foaming agent evolves gas at temperature at which polymer is liquid

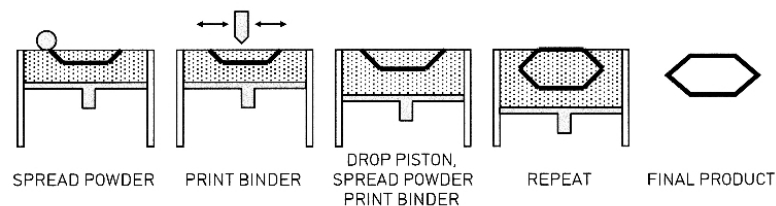
(b)

FREEZE-CASTING



(c)

RAPID PROTOTYPING



(d)

Gibson, L. J., M. Ashby, et al. *Cellular Materials in Nature and Medicine*. Cambridge University Press, © 2010. Figures courtesy of Lorna Gibson and Cambridge University Press.

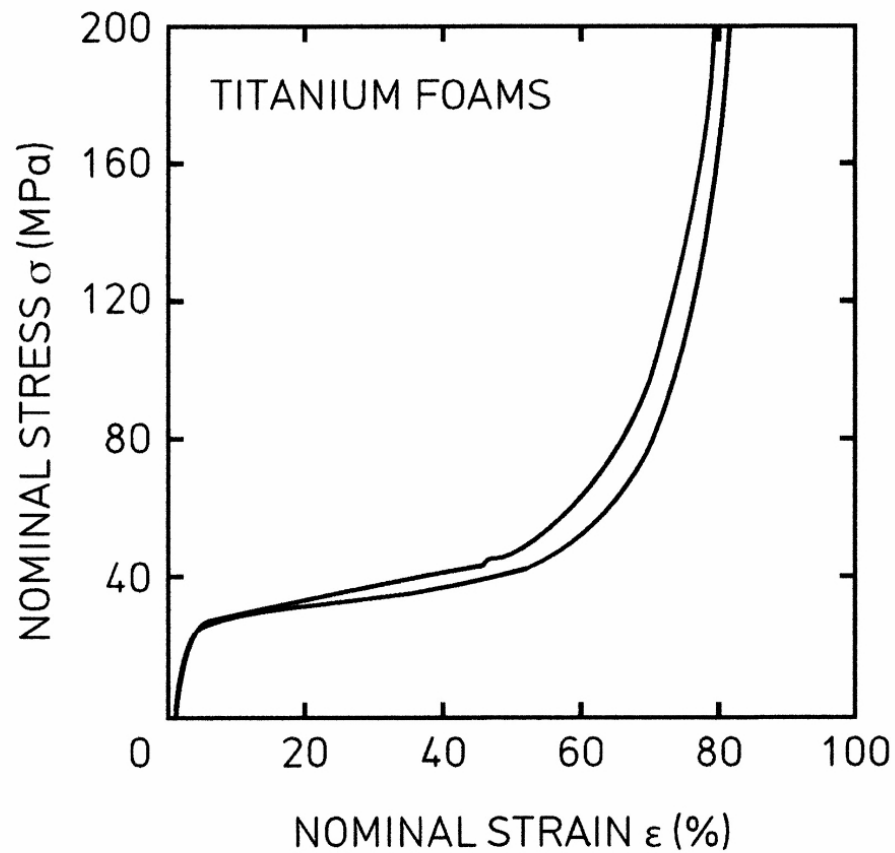
Processes

- (d) Expansion of foaming agent
- (e) Freeze casting (freeze dying)
- (f) Rapid prototyping (3D Printing, selective laser sintering)

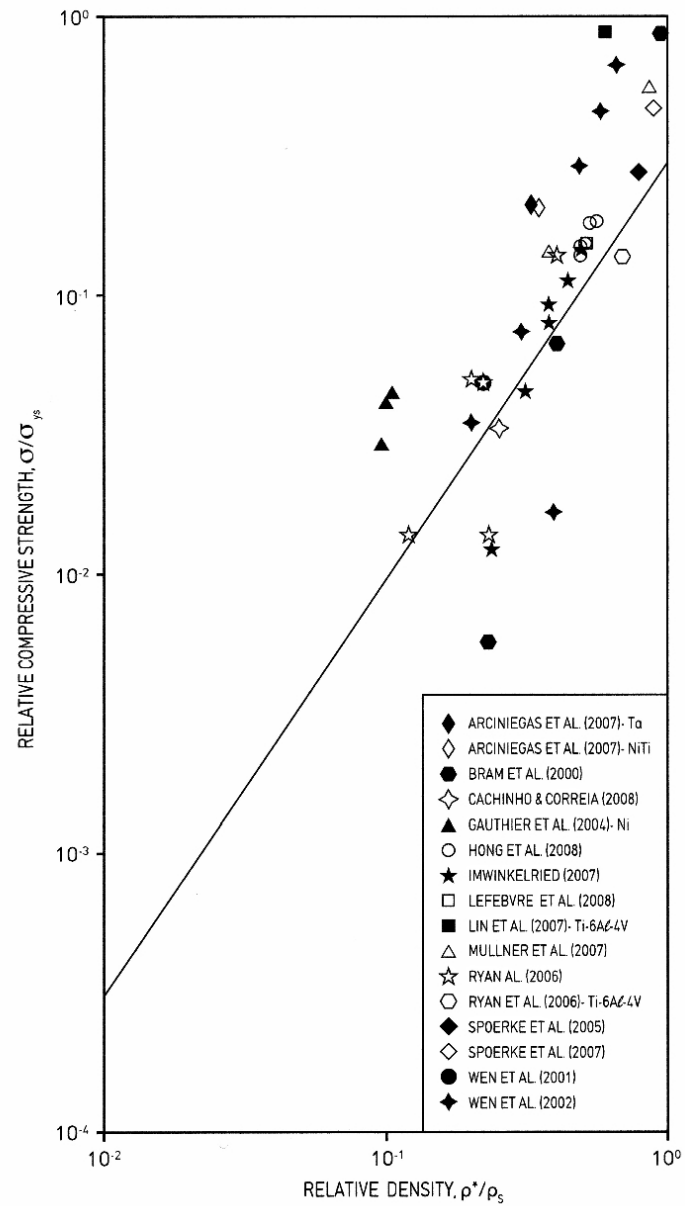
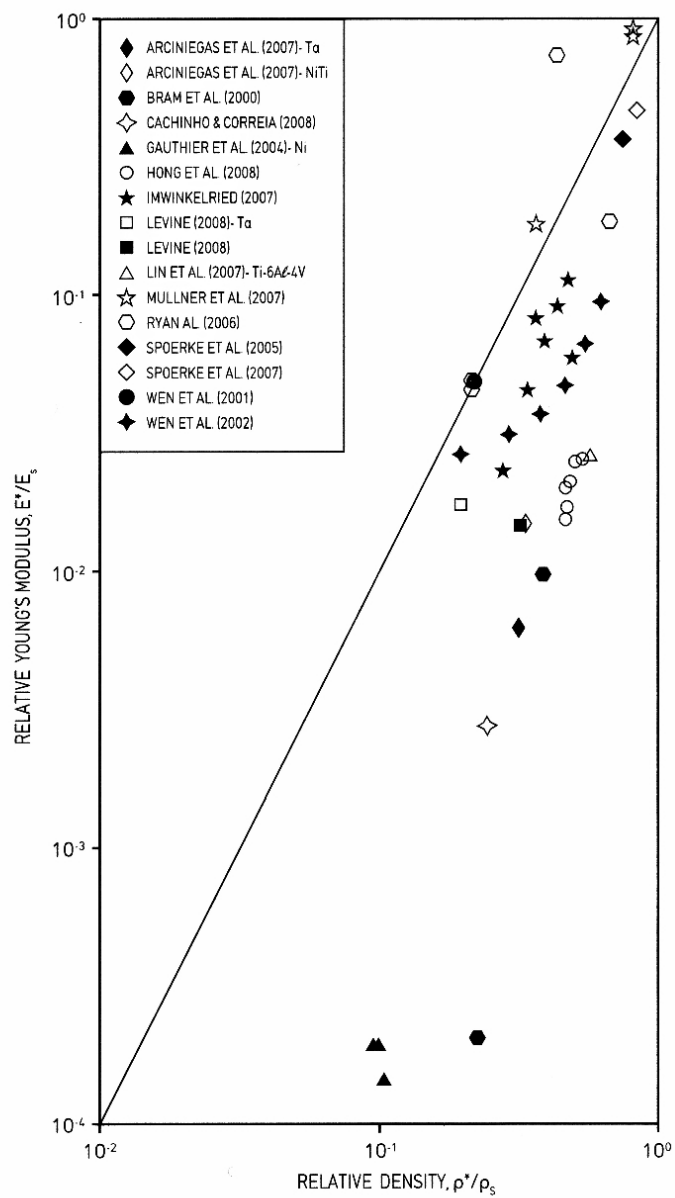
$\sigma - \epsilon$ curves - similar to other foams

Data for E^* , σ_c^*

Ti Foam: Stress-strain



Source: Wen, C. E., M. Mabuchi, et al. "Processing of Biocompatible Porous Ti and Mg." *Scripta Materialia* 45 (2001): 1147-53. Courtesy of Elsevier. Used with permission.



Gibson, L. J., M. Ashby, et al. *Cellular Materials in Nature and Medicine*. Cambridge University Press, © 2010. Figures courtesy of Lorna Gibson and Cambridge University Press.

Bone in Evolutionary Studies

Bone structure in evolutionary studies

- Phylogenetic chart — big picture — structural biomaterials (mineralized)
- Sponges — first multi-celled animal
 - calcarea: CaCO_3 spicules (needles)
 - hexactinellida: SiO_2 — “glass sponges”
 - demospongiae: most sponges — some have SiO_2 spicules
— spongin (type of collagen)
- Cnidarians - e.g. corals, jellyfish
 - Corals CaCO_3
- Mollusca — bivalves, snails, octopus
 - if mineralized CaCO_3
- Arthropods e.g. hexapoda (insects), arachnide (spiders), crustaceans (shrimp, lobster)
 - Exoskeleton of insects and spiders: chitin
 - Crustaceans: chitin may be mineralized with CaCO_3

Vertebrates

- Cyclostomata
 - jawless fish — lampreys hagfish
 - no vertebra — notochord
 - no bone
- Chondrichthye
 - sharks, rays, skates
 - cartilagenous skeleton — some mineralization, but not true bone
- Actinopterygii
 - ray-finned fish
 - true bone
 - 450 million years ago

Bone structure and loading

- Bone grows in response to loading
- Bone structure reflects mechanical loading and function; e.g. quadruped vs. biped
- Evolutionary studies have looked at trabecular bone architecture and density

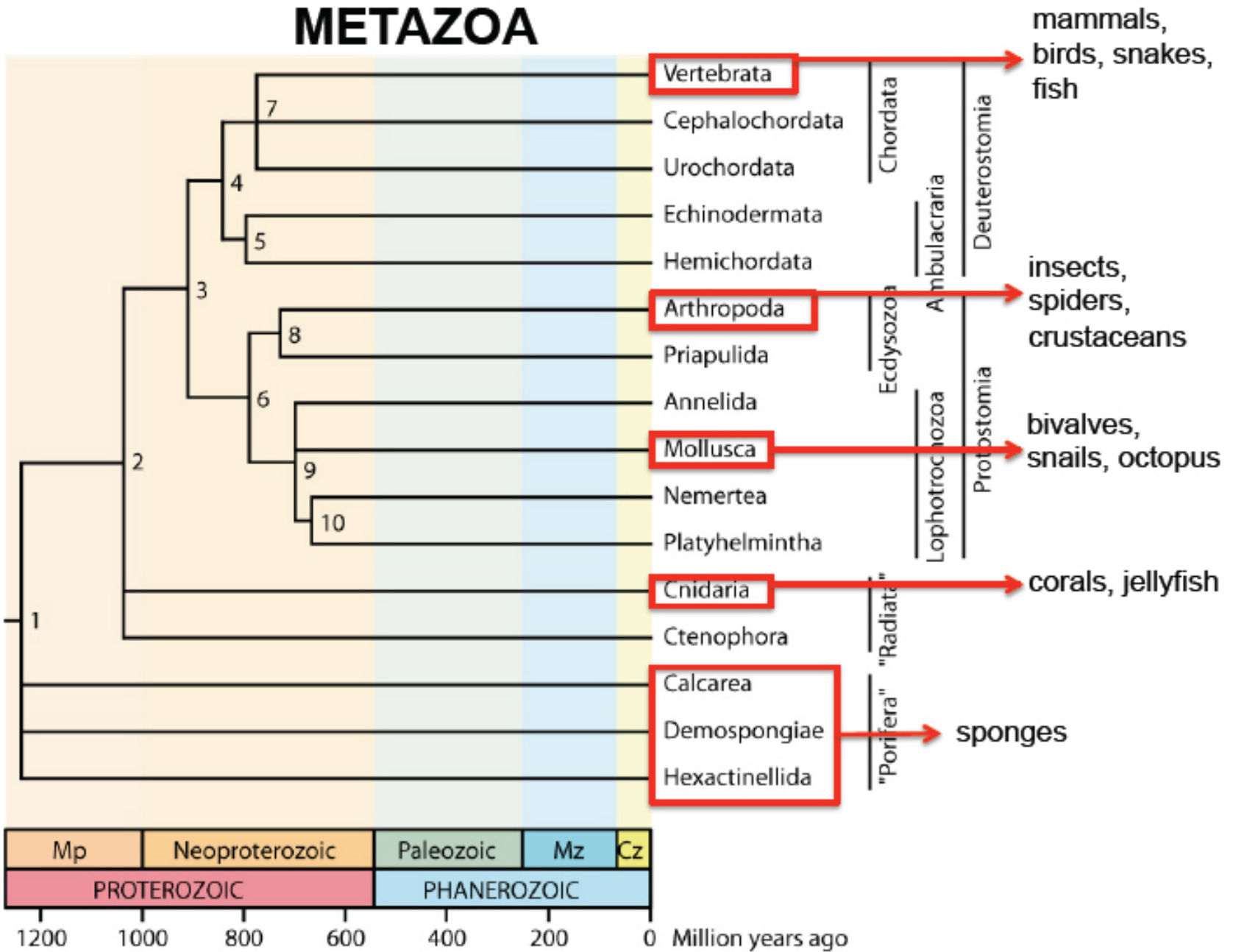


Fig. 2 A timetree of metazoan phyla. Divergence times are shown in Table 1. Abbreviations: Cz (Cenozoic), Mp (Mesoproterozoic), and Mz (Mesozoic).

Hedges and Kumar, 2009

From: *The Timetree of Life*. Hedges, S. B., and S. Kumar (eds.) © 2009 Oxford University Press. All rights reserved. This content is excluded from our Creative Commons license. For more information, see <http://ocw.mit.edu/help/faq-fair-use/>.



Venus Flower Basket (*Euplectella aspergillum*)

- Hierarchical structure
- Remarkably stiff, tough
- Joanna Aizenberg (Harvard)
- Aizenberg et al (2004) Biological glass fibers: correlation between optical and structural properties. PNAS

VERTEBRATA

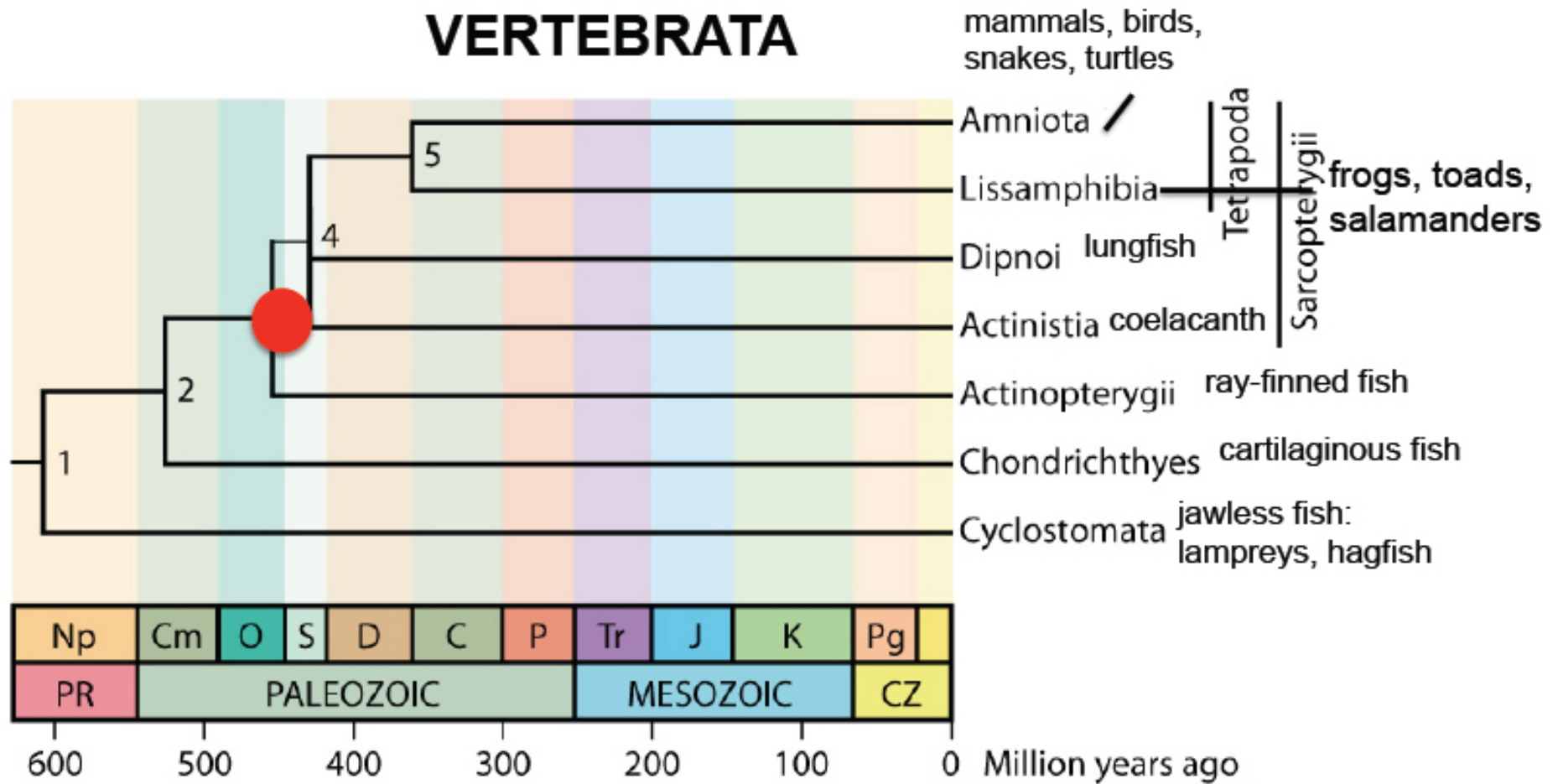


Fig. 2 A timetree of vertebrates. Times of divergence are averages of estimates from different studies listed in Table 1. Abbreviations: C (Carboniferous), Cm (Cambrian), CZ (Cenozoic), D (Devonian), J (Jurassic), K (Cretaceous), Np (Neoproterozoic), O (Ordovician), P (Permian), Pg (Paleogene), PR (Proterozoic), S (Silurian), and Tr (Triassic).



Common ancestor of all boned vertebrates roughly 450 MYA

(Hagfish video)

From: *The Timetree of Life*. Hedges, S. B., and S. Kumar (eds.) © 2009 Oxford University Press. All rights reserved. This content is excluded from our Creative Commons license. For more information, see <http://ocw.mit.edu/help/faq-fair-use/>.

Hedges and Kumar, 2009

Trabecular bone studies in human evolution

Oreopithecus bambolii (Rook et al, 1999)

- 7-9 Million years ago, late Miocene hominid, found in Italy
- Quadruped or biped?
- Compared trabecular architecture in ilium in apes, o. bambolii, humans
- Only had two fragments of ilium — left and right
- Took radiographs of both and digitally reconstructed a single ilium

Comparisons

- (a) Posterosuperior margin — marginal handles thicker than apes
- (b) Anterosuperior margin — iib bundle relatively structured compared to apes
- (c) Anteroinferior margin — well-developed a-i spine not seen in apes
- (d) Supra acetabular area — high density region
 - Collectively, observations suggest O. bambolii trab. architecture in ilium more similar to humans than apes
 - Suggests habitual bipedal locomotion (humans — obligatory bipeds)

Oreopithecus bambolii: Ilium

Rook et al. (1999)

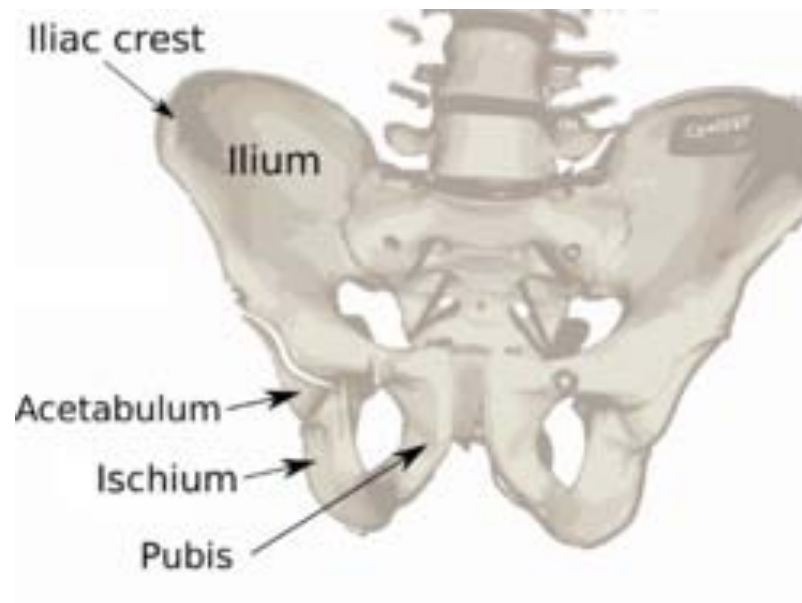


Image is in the public domain. Source: [Wikimedia Commons](#).

http://en.wikipedia.org/wiki/Iliac_crest

Trabecular architecture: Ilium

Figure removed due to copyright restrictions. See Figure 1: Rook L., et al. "[Oreopithecus was a Bipedal Ape after All.](#)" *Proceedings of the Natural Academy of Sciences* 96 (1999): 8795-99.

Digitally reconstructed ilium

Figure removed due to copyright restrictions. See Figure 2: Rook L., et al. "[Oreopithecus was a Bipedal Ape after All.](#)" *Proceedings of the Natural Academy of Sciences* 96 (1999): 8795-99.

Comparison of trabecular architecture

Figure removed due to copyright restrictions. See Figure 3: Rook L., et al. "[Oreopithecus was a Bipedal Ape after All.](#)" *Proceedings of the Natural Academy of Sciences* 96 (1999): 8795-99.

MIT OpenCourseWare
<http://ocw.mit.edu>

3.054 / 3.36 Cellular Solids: Structure, Properties and Applications
Spring 2014

For information about citing these materials or our Terms of Use, visit: <http://ocw.mit.edu/terms>.